Biophysical Journal

Supporting Material

Contributions of Ca^{2+}-Independent Thin Filament Activation to Cardiac Muscle Function

Yasser Aboelkassem,[1] Jordan A. Bonilla,[2] Kimberly J. McCabe,[1] and Stuart G. Campbell[1,*]

[1]Department of Biomedical Engineering, Yale University, New Haven, Connecticut; and [2]Department of Computing and Mathematical Sciences, California Institute of Technology, Pasadena, California

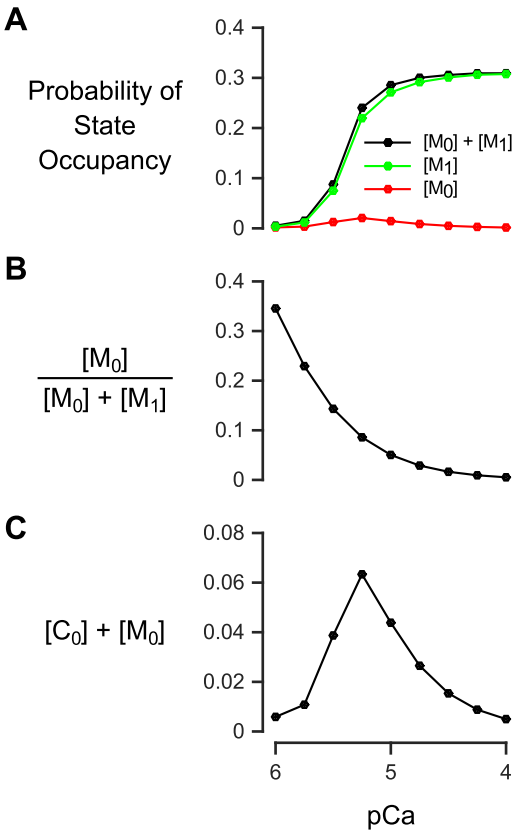

Supplemental Figure 1: Occupancy of the Ca^{2+}-independent states as a function of pCa, using Parameter Set 1, Table 1. (A) The probability of occupancy for the force-generating states M_0 and M_1 (and their sum). (B) The fraction of force arising from CIA (Ca^{2+}-independent activation), obtained by dividing the probability of the M_0 state by the total M-state probability ($[M_0] + [M_1]$). (C) The total probability of Ca^{2+}-free states (given by $[C_0] + [M_0]$).

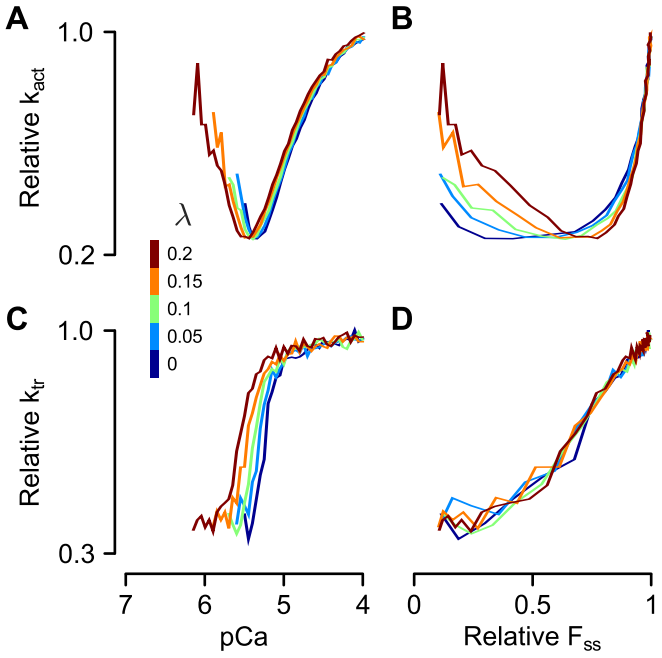

Supplemental Figure 2: The impact of Ca^{2+} and λ on rates of force development. Steady-state forces (F_{SS}) corresponding to each of the reported rate values are shown in Fig. 6A of the main manuscript. (A) The rate of force development following Ca^{2+} activation (k_{act}) is plotted as a function of pCa for λ values ranging from 0 to 0.2, as indicated by the color scale. (B) k_{act} values plotted as a function of steady-state force (F_{SS}). λ exerted complex effects on the k_{act}-F_{SS} relationship, speeding k_{act} at low forces but slowing it at force levels greater than 70% of maximum. (C) The rate of force re-development following slack/restretch (k_{tr}) as a function of both pCa and λ. (D) The same data plotted against F_{SS}. The exponential increase in k_{act} as it approaches maximum force (panel B) is reminiscent of measurements made in isolated cardiac myofibrils (41). A linear relationship between k_{tr} and F_{SS} (panel D) has been widely observed in skinned myocardial preparations (42, 43).

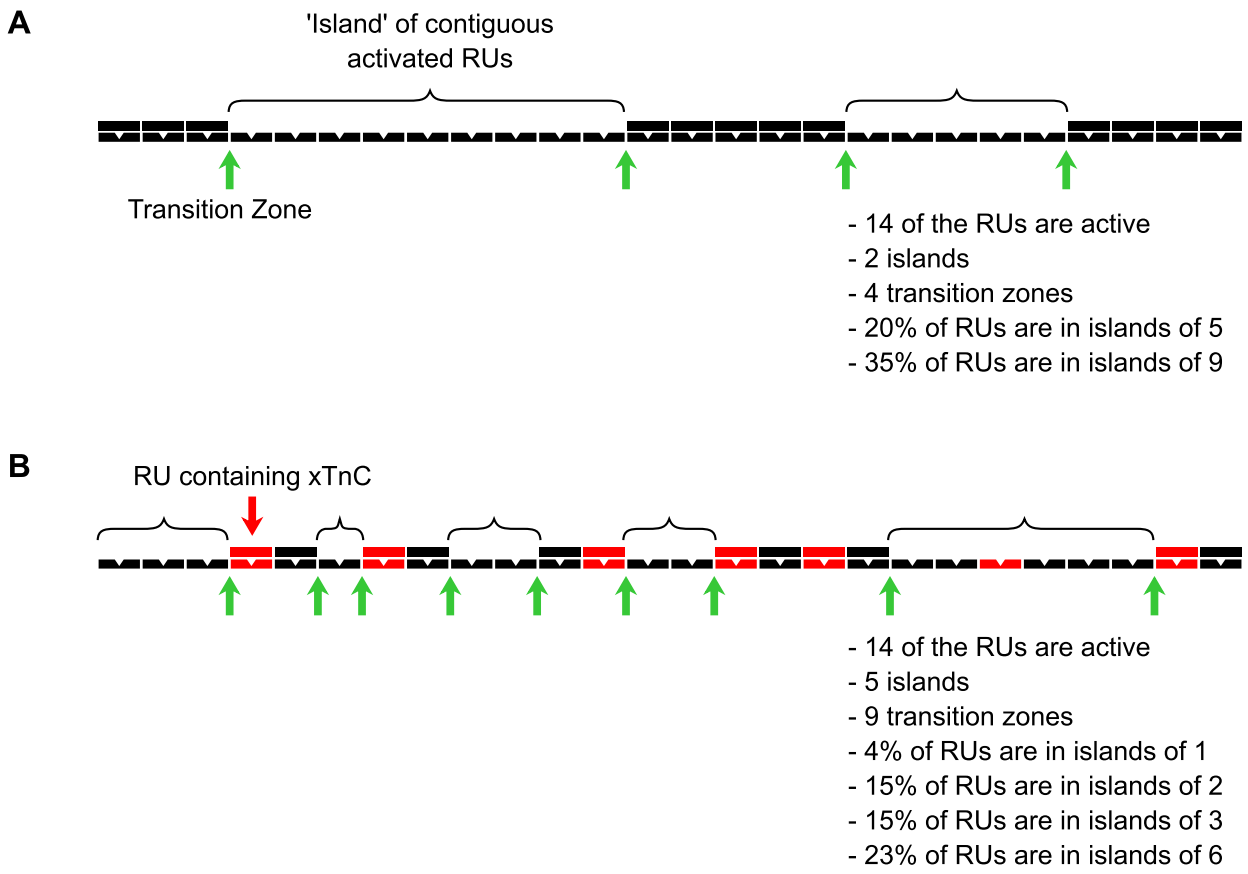

Supplemental Figure 3: Thin filament configurations and their characterization. The MCMC simulations performed in this study enabled characterization of patterns of thin filament activation under varying conditions. For instance, active RUs (C or M states) were frequently clustered together into 'islands' (panel A). By sampling many thin filament configurations from simulation data, it is possible to determine the statistical occurrence of islands of given sizes. This schematic also illustrates 'transition zones', which occur on either side of an island. At these points, adjacent RUs occupy dissimilar states (active vs. inactive). Under conditions of high Ca^{2+} and no xTnC (panel A), there are relatively few transition zones. When large numbers of RUs contain xTnC, activation islands become fragmented, and the number of transition zones drastically increases (panel B). Under conditions of high xTnC content, a model with fixed RU span, such as the one we employ here, tends to underestimate the steady-state force.

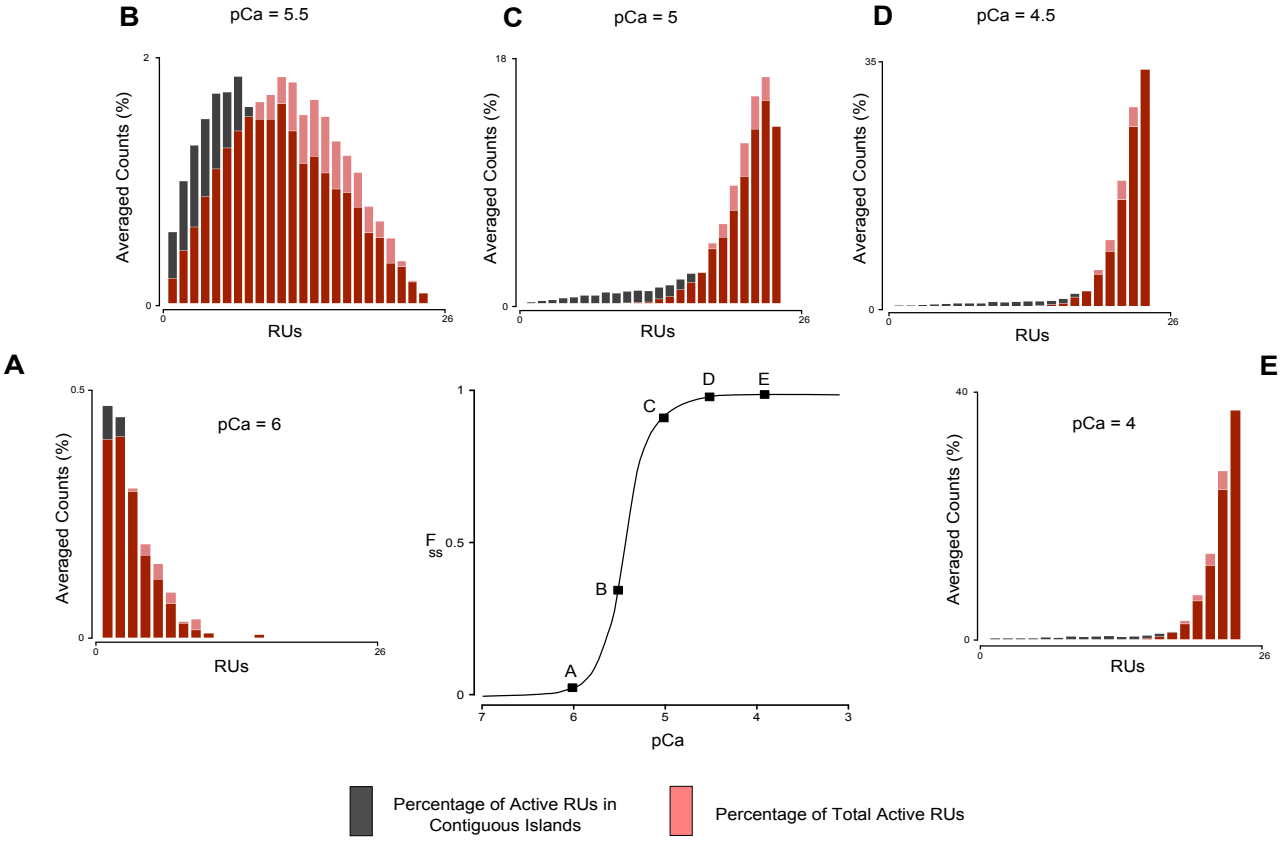

Supplemental Figure 4: Analysis of thin filament configurations predicted by the model. Many hundreds of thin filament configurations (see Supplemental Figure 3) were generated by the model at a range of pCa values, and were analyzed to determine the distribution of activation within filaments and across filaments. The inset in the center shows an F_{SS}-pCa curve produced by the model, with points labeled A-E). At each of these points, a histogram is shown that describes the sampled population of thin filament configurations. Red bars indicate the percentage of whole filaments having the total number of active RUs indicated by the bin on the x-axis. For instance, in panel A, the left-most red bar (the bin for 1RU) shows a value of ∼0.4%. This means that 0.4% of thin filaments sampled contained exactly 1 active RU. Black bars indicate how the active RUs are distributed within thin filaments. For example, the left-most black bar in panel A shows a value of ∼0.45%. This means that 0.45% of all RUs were found to be in islands 1 RU in length. Similarly, that same panel shows that detectable numbers of RUs were found in islands of length greater than 1 RU. We can see from this histogram that even at pCa 6, when activation is minimal, more RUs reside in contiguous islands (islands greater than 1 RU) than are activated in isolation (islands of 1). In panels B-E, it is clear that increasing Ca^{2+} concentration promotes the formation of larger and larger islands of active RUs.